CMCE

Computational Methods in Civil Engineering

Reliability analysis of suspension bridges against buffeting failure

S. Pourzeynali [a,*], T.K. Datta[b]

[a] *Department of Civil Engineering, Faculty of Engineering, University of Guilan, Rasht, Iran*
[b] *Department of Civil Engineering, Indian Institute of Technology, Huaz Khas, New Delhi- 110 016, India*

Abstract

A reliability analysis of suspension bridges against buffeting failure due to gustiness of wind velocity is carried out using the concept of PRA (probabilistic risk analysis) procedure. For this purpose, the bending stresses at the critical nodes of the bridge deck are obtained for buffeting forces using a spectral analysis technique and a finite element approach. For the purpose of reliability analysis, uncertainties are considered as those arising due to variation of stiffness and mass properties of the bridge, damping, mathematical modeling, flutter derivatives and due to ductility and damage concentration effects. These uncertainties are incorporated by a set of multiplying factors in the limit state function. All multiplying factors are assumed to be independent log-normally distributed random variables. An extensive parametric study is conducted to show the effect of some important parameters on the reliability estimate. The results of the study show that ductility of the system and the structural damping have a significant effect on the reliability against buffeting failure.

Keywords: Reliability analysis; Buffeting failure; PRA procedure; Suspension bridges; Ductility; Damage concentration.

1. Introduction

Earlier studies on wind induced vibration of suspension and cable stayed bridges relate to the determination of the flutter wind speed and buffeting response of the bridge deck [1-9]. A few of these studies also deal with the stability analysis of suspension bridges to wind induced excitations [10]. In recent years, Jain et al. [11] carried out a comprehensive study on the coupled flutter and buffeting analysis of long-span bridges by continuum approach using spectral analysis technique. The same concept was extended by Katsuchi et al. [12] to obtain the multimode coupled flutter and buffeting analysis of the Akashi-kaikyo Bridge in Japan. Compared to the dynamic response analysis of suspension bridges, reliability analysis of suspension bridges against dynamic phenomena is relatively less. Malla [13] presented a reliability analysis of cable-stayed bridges for seismic forces. Madsen and Rosenthal [14]

---
[*]Corresponding author. Fax No. +98-131-6690271.
E-mail address: pourzeynali@guilan.ac.ir (S. pourzeynali)

S. Pourzeynali, T.K. Datta / Comp. Meth. Civil Eng. 1 (2010) 15-35

16

carried out a study on the reliability analysis of the East Bridge, a suspension bridge with a main span of 1624 m, across the Great Belt in Denmark, against flutter wind speed. The study was done on the basis of measuring the critical wind speed values on a scale model in wind tunnel tests. Recently, Ge et al. [15] have applied a reliability analysis model to bridge flutter under extreme wind. They presented a reliability analysis model, which is formulated as a limit state up-crossing problem, and a probability calculation approach to determine the probability of bridge flutter due to wind. Authors [16] studied reliability analysis of suspension bridges against flutter failure. Not many studies are reported on the reliability of suspension bridges against buffeting. Since buffeting response of suspension bridges is one of the most important considerations in their design, it is desirable that the reliability of such bridges against buffeting failure is investigated thoroughly.

In this paper, the reliability of the suspension bridges against buffeting failure is presented using the concept of PRA (probability risk analysis) procedure and the basic reliability analysis method. For the purpose of reliability analysis, uncertainties are considered as those arising due to the variations of stiffness and mass properties of the bridge, damping, mathematical modeling, flutter derivatives and due to the ductility and damage concentration effects. These uncertainties are incorporated by a set of multiplying factors in the limit state function. All multiplying factors are assumed to be independent log-normally distributed random variables. The storm mean wind speed at the bridge site is assumed to follow type II distribution (given by Thom, [17]). A parametric study is conducted to show the effect of some important parameters on the reliability estimate. They include ductility of the system, threshold level, coefficients of variation of the damping factor, modeling factor, etc.

2. Assumptions

The following assumptions are made in the analysis:

1. Bridge deck is considered as a simply supported beam in each span. Therefore, it is assumed that bridge deck will fail if only one hinge occurs along any span.
2. The buffeting response of the bridge is a stationary Gaussian process with zero mean value.
3. In the reliability analysis against buffeting response failure, the probability of exceedance of the bending stress (beyond a specified threshold level) at the critical nodes along the bridge span, caused by fluctuating component of the wind velocity, from a specified threshold level is evaluated.
4. All stresses in the bridge elements obey the Hooke's law, and therefore no material non-linearity is considered.
5. The initial dead load is carried by cables without causing any stress in the suspended structure.
6. The cable is assumed to be of a uniform cross section and of a parabolic profile under dead load such that the weight of the cable can be assumed to be uniformly distributed along the span instead of along the length of the cable.
7. The hangers (or suspenders) are assumed to be vertical and inextensible, and their forces are considered to be distributed loads as if the distance between the suspenders is very small.
8. The original shape of every cross-section of the bridge deck is unaltered during vibration although the section may undergo out-of-plane deformation (Warping).
9. It is assumed that there is no tower resistance to displacement at the tower top and so the horizontal components of the cable tension H_w, (due to dead load) and h(t), (due to dynamic load) are the same on both sides of the tower.

S. Pourzeynali, T.K. Datta / Comp. Meth. Civil Eng. 1 (2010) 15-35

17

3. Equation of motion

The buffeting response of suspension bridge is evaluated using finite element method (FEM) by coupled multi-mode analysis. For this purpose, the bridge deck is discretized into two-dimensional beam elements each consisting of two nodes at its ends. At each node, four degrees of freedom, as shown in Figure 1 are considered. The dynamic degrees of freedom are taken as the vertical (q_1^V and q_3^V) and torsional (q_1^θ and q_3^θ) degrees of freedom and therefore, the rotational (q_2^V and q_4^V) and torsional (q_2^θ and q_4^θ) degrees of freedom are condensed out from the overall stiffness matrix.

The wind induced aerodynamic (self-excited and buffeting) forces can be lumped at both ends of each element as shown in Figures 2 c and d. The aerodynamic forces per unit length of the bridge span (Figures 2 a and b) may be separated into two parts as [11]
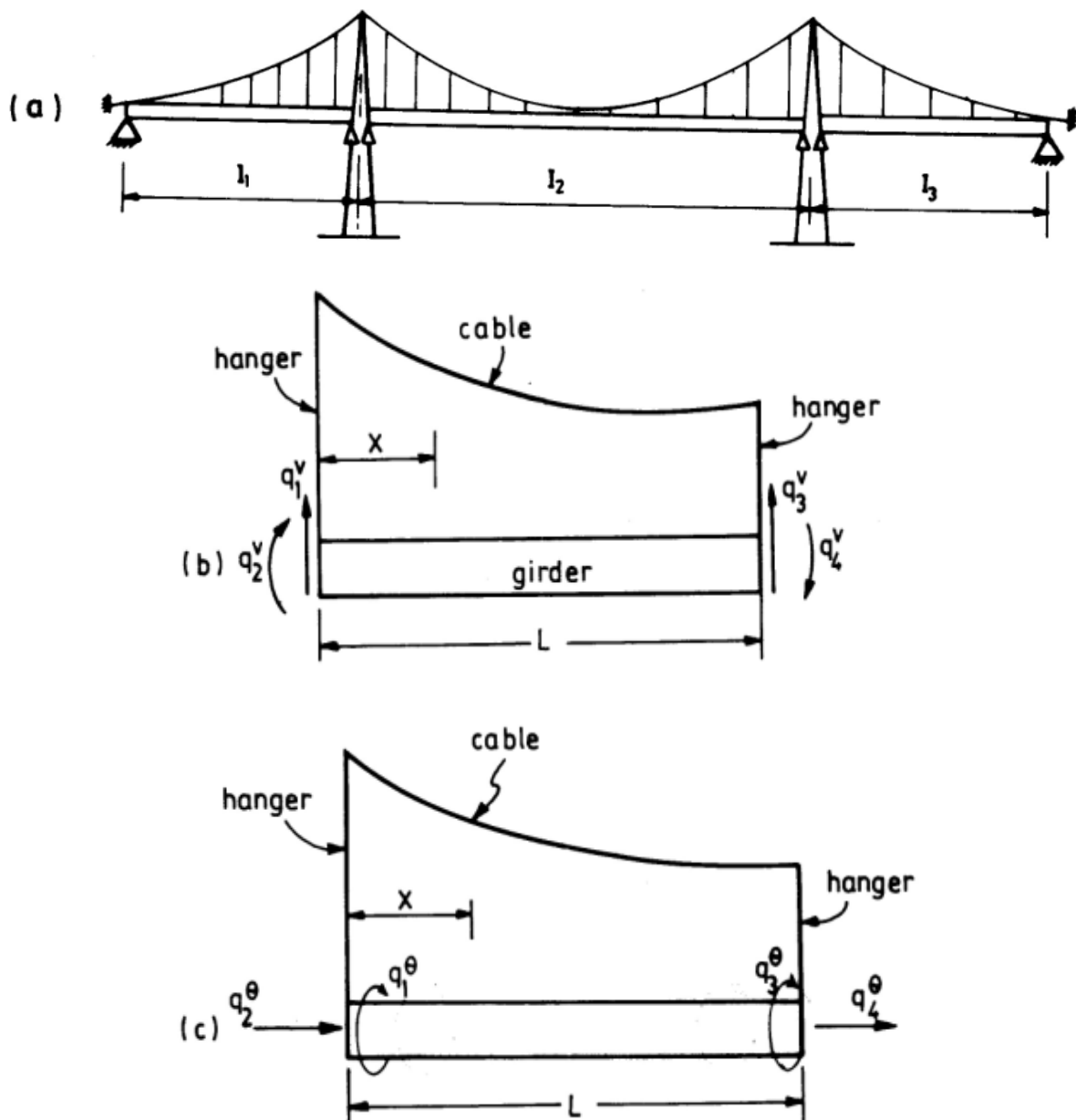
$$L = L_{ae} + L_b \tag{1a}$$

Figure 1. Suspension Bridge model: (a) schematic view; (b) flexural deformations at the ends of bridge deck element; and (c) torsional deformations at the ends of bridge deck element.
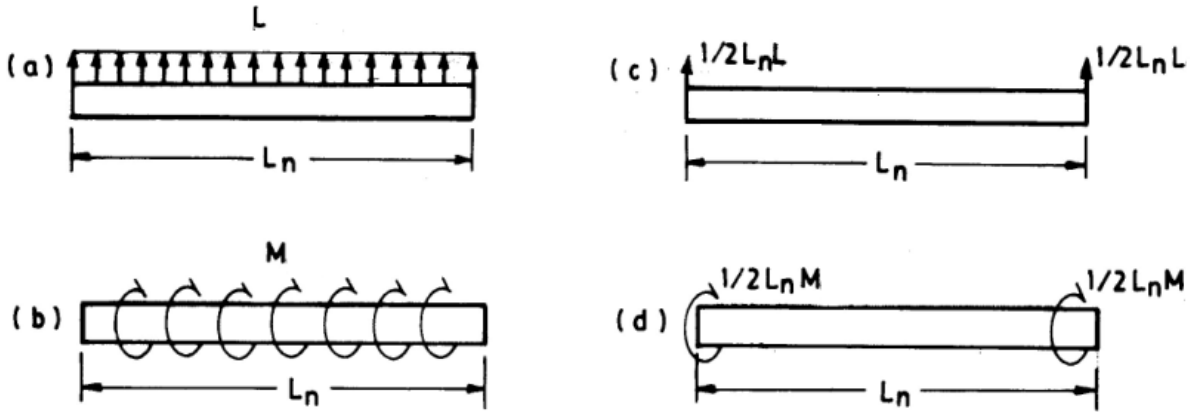
Figure 2. Aerodynamic forces: a) Distributed vertical load; b) Distributed torsional moment;
c) Lumped vertical load; d) Lumped torsional moment.

$$M = M_{ae} + M_b \qquad (1b)$$

where L is the lift force and M is the torsional moment, respectively; and ae refers to aeroelastic and b refers to buffeting forces. Detail descriptions of these forces are provided in references [18-20].

The governing equation of motion in the matrix format can be written as

$$[M]\{\ddot{x}\} + [C]\{\dot{x}\} + [K]\{x\} = \{F\}_{ae} + \{F\}_b \qquad (2)$$

where $[M]$ is the lumped mass matrix of size $2n \times 2n$; $[C]$ is the structural damping matrix of size $2n \times 2n$; $[K]$ is the condensed structural stiffness matrix of size $2n \times 2n$; and $\{x\}$ is the $(2n \times 1)$ displacement vector defined as

$$\{x\} = \{v_1, v_2 ..., v_n, \ \theta_1, \theta_2, ... \theta_n\}^T_{1 \times 2n} \qquad (3)$$

in which v_i *and* θ_i are the vertical and torsional displacement at node i along the bridge span, respectively; and n is number of nodes along the bridge span. The condensed stiffness matrix $[K]$ is derived from a $4n \times 4n$ stiffness matrix $[\overline{K}]$ of the form

$$[\overline{K}] = \begin{bmatrix} \overline{K}^V & / & 0 \\ -- & / & -- \\ 0 & / & \overline{K}^\theta \end{bmatrix} \qquad (4)$$

in which $\overline{K}^V$ *and* $\overline{K}^\theta$ are bending and torsional stiffness matrices respectively, each of size $2n \times 2n$. Elemental bending stiffness (corresponding to the degrees of freedom q_1^V, q_2^V, q_3^V *and* q_4^V) and torsional stiffness (corresponding to the degrees of freedom $q_1^\theta, q_2^\theta, q_3^\theta$ *and* q_4^θ) matrices are derived from energy principles in which cable/ structure strain energies are only considered [21, 22].

$\{F\}_{ae}$ and $\{F\}_b$ are the self-excited and buffeting force vectors, given in references [18, 19]. Solution of the equation(2) using a standard random vibration spectral analysis in frequency domain [23], provides the power spectral density functions of buffeting responses (both displacement and bending moment) at the nodes of the bridge.

4. Probabilistic description of wind
4.1. Probabilistic description of wind gustiness

In random vibration analysis of the structures due to fluctuating component of wind velocity (also called gustiness of the wind), the power spectral density function (PSDF) of the gustiness of wind is required as an input. Various empirical models for describing the PSDF

S. Pourzeynali, T.K. Datta / Comp. Meth. Civil Eng. 1 (2010) 15-35

19

of wind velocity (wind spectra) are available. In the present study the model proposed by Simiu and Scanlan [24] is used, which is given in Appendix-I.

4.2. Probabilistic description of storm mean wind speed

As it would be shown later, the probability of fatigue failure of suspension bridges depends on the storm mean wind speed at the site of the bridge. Therefore, for the evaluation of the reliability, the distribution of storm mean wind speed is needed. It is assumed that storm mean wind speed follows the Type II (Frechet) distribution given by Thom [17] as follows

$$F_u[U] = exp\left(-\left(\frac{U}{\beta}\right)^{-\gamma}\right) \tag{5}$$

$$f_u(U) = \frac{\gamma}{\beta}\left(\frac{U}{\beta}\right)^{-\gamma-1} exp\left[-\left(\frac{U}{\beta}\right)^{-\gamma}\right] \tag{6}$$

in which $F_u(U)$ and $f_u(U)$ are the CDF and PDF of the storm mean wind speed U, respectively; β is the scale parameter and γ is the tail length parameter.

As well, the effect of Gumbel type I distribution, as the distribution of storm mean wind speed, on reliability against buffeting failure is also investigated. The probability density (PDF) and distribution (CDF) functions of this distribution can be expressed as follows

$$f_u(U) = \overline{\alpha}\, exp\left[-\overline{\alpha}(U - \overline{u}) - exp\left\{-\overline{\alpha}(U - \overline{u})\right\}\right] \qquad -\infty \le U \le +\infty \tag{7}$$

$$F_u(U) = exp\left[-exp\left\{-\overline{\alpha}(U - \overline{u})\right\}\right] \qquad -\infty \le U \le +\infty \tag{8}$$

The parameters $\overline{u}$ (location) and $\overline{\alpha}$ (dispersion) are given by

$$U_{mean} = \overline{u} + \frac{0.5772}{\overline{\alpha}} \tag{9}$$

$$\sigma_U{}^2 = \frac{\pi^2}{6\overline{\alpha}^2} \tag{10}$$

where U_{mean} and σ_U are the mean and standard deviation of the storm mean wind speed U.

5. Reliability analysis

5.1. Uncertainties considered in the study

The uncertainties in geometric and material properties of the bridge and the construction defects finally lead to uncertainties in the mass, stiffness properties of the bridge. The other uncertainties that are considered include uncertainties in mathematical modeling, structural damping and flutter derivatives. All these uncertainties affect the dynamic characteristics of the bridge and hence, the buffeting response of the bridge. The uncertainties in mass and stiffness give rise due to uncertainties in modal characteristic of the bridge and therefore, they are incorporated separately by a simulation procedure. The uncertainties arising from damping, mathematical modeling and flutter derivatives are considered directly in the reliability limit state function.

5.1.1 Mass and stiffness uncertainties

The variation in the material and geometric properties of the bridge leading to the variations of the mass and stiffness properties of the system is complex and difficult to appropriately consider in the reliability analysis. The problem requires the mass and stiffness properties of the structure to be modeled as random variables leading to the use of stochastic finite element analysis or simulation procedure. In order to keep the present reliability analysis procedure simple and to obtain a preliminary estimate of reliability, the variation of

S. Pourzeynali, T.K. Datta / Comp. Meth. Civil Eng. 1 (2010) 15-35

20

the mass and stiffness properties of the bridge are considered by writing these matrices in the following form

$$[K_\rho]=\rho_1[K] \tag{11}$$
$$[M_\rho]=\rho_2[M] \tag{12}$$

in which $[K]$ and $[M]$ are the basic stiffness and mass matrices of the bridge, respectively, are considered as deterministic; ρ_1 and ρ_2 are log-normally distributed random variable factors which represent the variability of stiffness and mass matrices. In order to make this variation more general, the factor ρ_1 itself can be considered as a combination of three factors i.e.,

$$\rho_1 = F_1.F_2.F_3 \tag{13}$$

in which F_1 represents the effect of variability of modulus of elasticity (E) ; F_2 represents the uncertainty resulting from the variation of shear modulus (G) ; and F_3 represents the uncertainty resulting from bridge geometry. All these factors are considered as independent log-normally distributed random variables with a mean value of unity. The coefficient of variation (COV) of ρ_1 can be evaluated as [25]

$$1+\delta\rho_1^2 = \left(1+\delta_{F1}^2\right)\left(1+\delta_{F2}^2\right)\left(1+\delta_{F3}^2\right) \tag{14}$$

where $\delta\rho_1$ is the COV of the ρ_1, δ_{Fi} are the COV of the factors F_i (i=1-3).

Since some of the elements of the stiffness matrix contain the parameter 'E', while other elements contain the parameter 'G', the values of δ_{F1} and δ_{F2} may be considered as 0.5 δ_E and 0.5 δ_G; δ_E and δ_G are the COV of the parameters E and G, respectively. Thus equation (14) can be written as

$$1+\delta_{\rho1}^2 = \left(1+\left(0.5\delta_E\right)^2\right)\left(1+\left(0.5\delta_G\right)^2\right)\left(1+\delta_{F3}^2\right) \tag{15}$$

In a similar manner, $\delta\rho_2$ can be calculated, assuming that $\rho_2 = \mu F_3$ in which μ represents the variation of mass density of the material.

Since ρ_1 and ρ_2 are log-normally distributed random variables, mean values of these random variables can be related to their standard deviations. With the standard deviation and mean values of ρ_1 and ρ_2 as known, random values of ρ_1 and ρ_2 can be artificially generated, which are used in section 5.2 for reliability analysis against buffeting failure.

5.1.2. Damping, modeling, and flutter derivatives uncertainties

Buffeting response of the bridge deck, which are calculated according to the procedures given in previous sections, as would be seen later, are multiplied by three factors F_4, F_5, and F_6, in order to take in to account the uncertainties due to damping, modeling and flutter derivatives. These uncertainty coefficients are again considered as independent log-normally distributed random variables, with mean value of unity.

There are very few data available from the measured structural damping of suspension bridges, which show the damping variability. According to Davenport [26], the structural damping of the long span suspension bridges can be expressed as

$$\zeta_\theta = \frac{c}{n}E \tag{16}$$

where ζ_θ is the torsional mode damping ratio to critical; n is structural frequency (Hz); c is the proportionality coefficient; E is a log-normally distributed random factor with mean value of unity and coefficient of variation to be 0.40. Since the buffeting response of suspension bridges change with the damping ratio ζ_θ, the effect of the C.O.V. of the factor F_4 (δ_{F4}) on the buffeting response is investigated with the upper limit of δ_{F4} as 0.40.

The actual bridge structure is always more complicated than its simplified model which is considered for analysis. For example, the three-span suspension bridge is considered here as a

S. Pourzeynali, T.K. Datta / Comp. Meth. Civil Eng. 1 (2010) 15-35

21

three-span simply supported beam. Also, some other assumptions and simplifications are made during the study, which introduce some uncertainties in the evaluation of the buffeting response. These uncertainties are incorporated in the analysis by considering a C.O.V. of the factor F_5 (δ_{F5}) as 0.10.

Factor F_6 accounts for the uncertainties arising from the insufficient knowledge of flutter derivatives. In this study, flutter derivatives are estimated from experimentally given curves by Scanlan and Tomko [27], which were measured under zero angle of attack and low speed flow (laminar flow). Thus, the effects of actual turbulence of wind flow and wind direction are not considered in the analysis. In addition, experimental error and curve fitting techniques introduce extra uncertainties for the values of flutter derivatives used in the analysis. According to a study [24] disparity between the results of flutter derivatives obtained under turbulent and laminar conditions, especially for A_2^* [18-20], for reduced velocities $U/(nB) < 12$ [18-20] is of the order of 15%. Keeping the above in view, the COV for factor F_6 (δ_{F6}) is taken as 0.20.

5.2. Reliability analysis against buffeting response failure

As was explained in previous sections, the buffeting response of suspension bridges is calculated using the spectral analysis method in frequency domain. The resulting responses may be affected by the associated errors in evaluating the material properties, damping of the system, modeling of the problem and flutter derivatives. Thus, the uncertainties should be properly considered in the analysis. In the reliability analysis, the failure of the structure is defined as

$$g(X) = R - S < 0 \tag{17}$$

In general, the variables R and S are called resistance and load effect of the system and are functions of a number of basic random variables. In this part of study for evaluating the reliability against buffeting failure, S may be written as

$$S = (k \, \sigma_x) \, F_m. \, F_4.F_5.F_6 \tag{18}$$

where the factors F_4, F_5 and F_6 are defined in previous sections; F_m is an independent log-normally distributed random variable which is considered to incorporate the material uncertainty into the buffeting responses; σ_x is the RMS value of the bending stress at the critical nodes of the bridge (Figure 3) for which the reliability analysis is being performed and is considered as deterministic; and k is the peak factor of the bending stress given as [28]

$$k = (2 \, ln \, \upsilon T)^{\frac{1}{2}} + \frac{0.5772}{(2 \, ln \, \upsilon T)^{\frac{1}{2}}} \tag{19}$$

$$\upsilon = \left\{ \frac{\left[\int_0^\infty n^2 \, S(n) \, dn\right]^{\frac{1}{2}}}{\int_0^\infty S(n) \, dn} \right\} \tag{20}$$

in which n is the natural frequency (Hz); $S(n)$ is the **PSDF** of the stress; and T is duration of the process.

S. Pourzeynali, T.K. Datta / Comp. Meth. Civil Eng. 1 (2010) 15-35
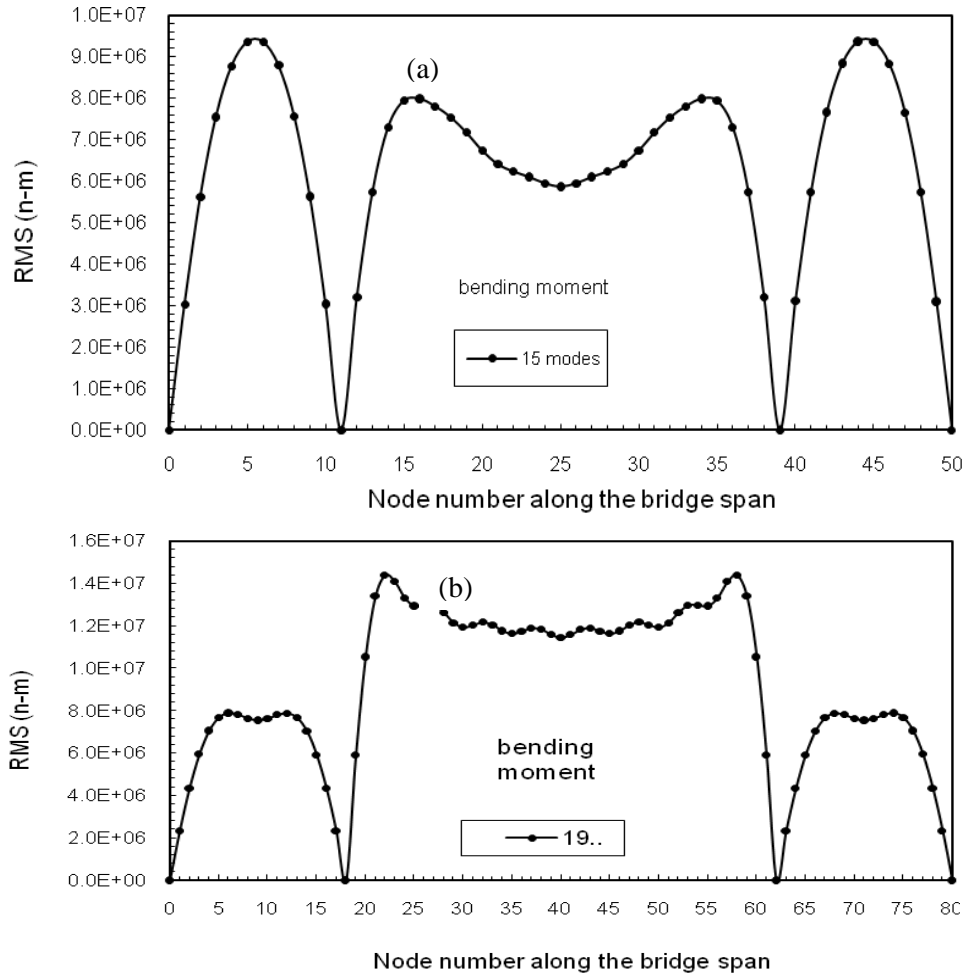
22

Figure 3. RMS values of the bending moment along the bridge span: a) Thomas Bridge;
b) Golden Gate Bridge.

As was explained in the previous sections, the material uncertainties were incorporated using the random coefficients ρ_1 and ρ_2 and by using a simulation procedure. In the buffeting reliability analysis, the long hand simulation to obtain the mean and standard deviation of the buffeting response is computationally very intensive. Therefore, the material uncertainty in the buffeting response is incorporated by considering an additional random variable factor F_m in equation (18). The median value of F_m is taken as unity and the logarithmic standard deviation (σ_{lnFm}) can be calculated using the ratio between 84th percentile non-exceedance and the median response as given by Takeda et al. [29]

$$\sigma_{lnFm} = ln\frac{\sigma_{84}}{\sigma_{50}} \tag{21}$$

in which σ_{50} is the bending stress (RMS value) corresponding to the median values of coefficients ρ_1 and ρ_2; and σ_{84} also is the bending stress corresponding to the median $+1\sigma$ of the coefficients ρ_1 and ρ_2. σ_x in equation (18) is obtained for the median values of ρ_1 and ρ_2. Note that the bending stresses are obtained using the $[K_\rho]$ and $[M_\rho]$ matrices defined in equations (11) and (12), in which the appropriate values of ρ_1 and ρ_2 as described above are used.

Further, the resistance (R) of the limit state equation (equation (17)), takes the form

$$R=C.F_7.F_8 \tag{22}$$

where C is the capacity of the structure which is considered to resist the fluctuating component of the bending stress, and is assumed to be a percentage of yield stress σ_y. F_7 is

S. Pourzeynali, T.K. Datta / Comp. Meth. Civil Eng. 1 (2010) 15-35

23

the ductility factor, which represents inelastic energy absorption, and its median value can be calculated using Numark's formula, $\sqrt{2\mu - 1}$, and is reduced to about 60% of the formula [29] in which μ is the ductility factor. The concept of factor F_7 is useful for single-degree-of-freedom systems, but in order to represent the damage concentration effect of MDOF systems, the factor F_8 is used. Median value of F_8, as shown by Takeda et al. [29], can vary from 0.75 to 2.

In equations (18) and (22), all the random variables are assumed to be independent log-normally distributed. Therefore, the variables R and S would be log-normal, and for calculating the probability of failure, P_f, first order and second moment (FOSM) method can be used. The procedure is given in the following:

$$P_f = P\left(g(X) < 0\right)$$
$$= P\left(R < S\right)$$
$$= P\left(R/S < 1\right) \tag{23}$$

let $\quad Z = R/S \tag{24}$

Since R and S are independent and log-normally distributed, then Z also is log-normally distributed and its logarithmic mean and standard deviation are given as

$$\mu_{lnZ} = ln\left(\tilde{Z}\right) = ln\left(\frac{\tilde{R}}{\tilde{S}}\right) \tag{25}$$

$$\sigma_{lnZ} = \sqrt{\sigma_{lnR}^2 + \sigma_{lnS}^2} \tag{26}$$

Since $\tilde{F}_7 = \sqrt{2\mu - 1} \times 0.60$ as described previously,

$$\tilde{R} = \tilde{C} \cdot \tilde{F}_7 \cdot \tilde{F}_8 = \left(\bar{\gamma}\,\sigma_y\right)\left(\sqrt{2\mu - 1}\right) \times 0.60 \times \tilde{F}_8 \tag{27}$$

$$\tilde{S} = \left(k\,\sigma_x\right)\tilde{F}_m \cdot \tilde{F}_4 \cdot \tilde{F}_5 \cdot \tilde{F}_6 = k\,\sigma_x \tag{28}$$

$$\sigma_{lnR}^2 = ln\left(1 + \delta_R^2\right) \quad , \quad \sigma_{lnS}^2 = ln\left(1 + \delta_S^2\right)$$

$$\tag{29}$$

$$1 + \delta_R^2 = \left(1 + \delta_C^2\right)\left(1 + \delta_{F7}^2\right)\left(1 + \delta_{F8}^2\right) \tag{30}$$

$$1 + \delta_S^2 = \left(1 + \delta_{Fm}^2\right)\left(1 + \delta_{F4}^2\right)\left(1 + \delta_{F5}^2\right)\left(1 + \delta_{F6}^2\right) \tag{31}$$

in which over hat denotes the median value; and $\bar{\gamma}$ is the ratio of capacity C to the yield stress σ_y. The probability of failure P_f for a single storm may be expressed as

$$P_f = P\left(ln\,Z < 0\right)$$

$$= \Phi\left(\frac{0 - \mu_{lnZ}}{\sigma_{lnZ}}\right)$$

$$= \Phi\left(-\beta\right) \tag{32}$$

where Φ is standard normal distribution function and

$$\beta = \frac{\mu_{lnZ}}{\sigma_{lnZ}} \tag{33}$$

As the buffeting response of the bridge depends on the mean wind velocity during the storm, P_f can be weighted by the annual probability density function of the storm mean wind velocity $f_u(U)$, given by Thom [17] in the range of interest as

$$P_E = \int_U P_f \cdot f_u\left(U\right) dU \tag{34}$$

Thus, if the number of storms in one year is assumed to be $\bar{n}$, the probability of failure during $\bar{m}$ years of lifetime of the bridge can be expressed as

$$P_{\bar{m}\bar{n}} = 1 - \left(1 - P_E\right)^{\bar{m}\bar{n}} \tag{35}$$

6. Numerical studies

As numerical examples, the Thomas Suspension Bridge located between San Pedro and Terminal Island in Los Angeles County, California; and the Golden Gate Suspension Bridge located in San Francisco, California, are chosen. For these three-span suspension bridges, the structural data are taken from the literature [21, 22, 27]. Some of the structural data are given in the following:

For Thomas Bridge: (1) one center span l_2=460 m; (2) two side spans l_1=l_3=155m; (3) dead load of the bridge w=52438.020 N/(m-cable); (4) cross-sectional area of one cable, A_c=0.0780 m^2; (5) moment of inertia of bridge deck for center span I_2=0.7258 m^4, and for side spans I_1=I_3=0.7498 m^4.

For Golden Gate Bridge: (1) one center span l_2=1280.6 m; (2) two side spans l_1=l_3=342.9m; (3) dead load of the bridge for center span w_2=166982.3 N/(m-cable), and for side spans w_1=w_3=168440.7N/(m-cable); (4) cross-sectional area of one cable, A_c=0.5367 m^2; (5) moment of inertia of bridge deck for center span I_2=5.4346 m^4, and for side spans I_1=I_3=3.4285 m^4.

The results of the free vibration analyses for both bridges which provide the modal properties of the bridges are given in references [16, 18].

As mentioned before, the bending stresses are calculated at the critical nodes corresponding to the median values of the coefficients ρ_1 and ρ_2 (σ_{50}) and median + 1σ of these coefficients (σ_{84}) for both bridges. Node 5 and node 22 (Figure 3) are considered as the critical nodes for Thomas and Golden Gate Bridges, respectively, for which the values of δ_{Fm} are evaluated as 7.4% and 26.5%. In order to obtain the probability of failure due to bending stress, the mean value of factors F_4, F_5 and F_6 are taken as unity and the coefficients of variation δ_{F4}, δ_{F5} and δ_{F6} are taken as 0.40, 0.10 and 0.20, respectively. The range of mean wind speed is considered from 15 to 55 m/sec and 10 to 32 m/sec for Thomas and Golden Gate Bridges, respectively. Note that for suspension bridges the range of mean wind speed is limited by the flutter speed. In this study, the flutter speed for Thomas Bridge is considered about 58.22 m/sec (obtained from another study by authors), and that of the Golden Gate Bridge about 33.39 m/sec. By taking the above in view, the parameters of the wind distribution (given by Thom [17]) are chosen as γ=5 and β=20 for Thomas Bridge, and γ=7 and β=18 for Golden Gate Bridge. The ductility factor μ is taken as 4 and the median value of factor F_8 as 1.25. The yield stress for the steel material of the bridge deck (σ_y) is assumed to be about 2.4×10^8 N/m^2.

The probability of failure (P_f) due to bending stress is calculated using the FOSM method (equation (32)) by assuming that all random variables are log-normally distributed. P_f is calculated for different values of the mean wind speed. The capacity C, to resist bending stress at the critical nodes is taken about 20%, 33% and 50% of σ_y. The results are shown in the Figures 4a and 4b for Thomas and Golden Gate Bridges, respectively. It can be seen from the figures that the capacity C has a significant effect on the reliability against buffeting failure. As C increases, reliability also rapidly increases. Further, reliability decreases with the increase in the value of the mean wind speed U.

The variation of reliability versus mean wind speed U at the critical node of the center span for Thomas Bridge (node 16) and at the critical node of the side span for Golden Gate Bridge (node 5) is shown in Figures 5a and 5b, respectively. For these nodes also, reliability varies in the same manner as that of the other critical nodes.

The effect of some important parameters such as wind distribution, ductility factor, damping ratio, etc. on the reliability against buffeting failure is investigated through a parametric study. The results are given in the following.
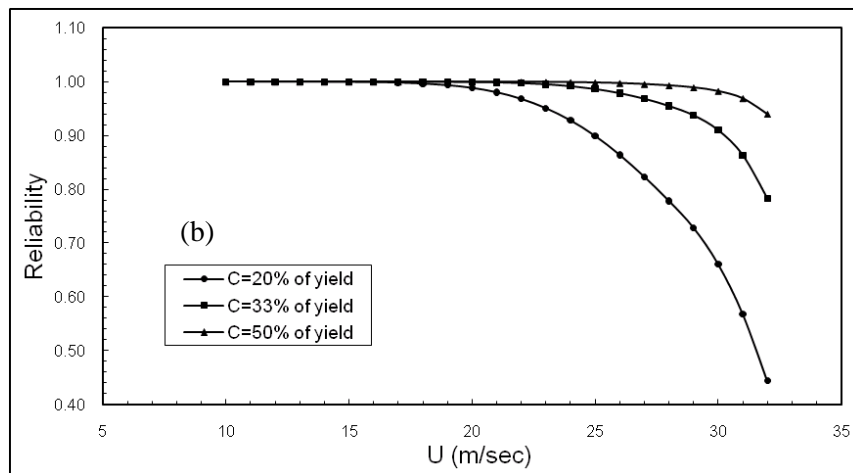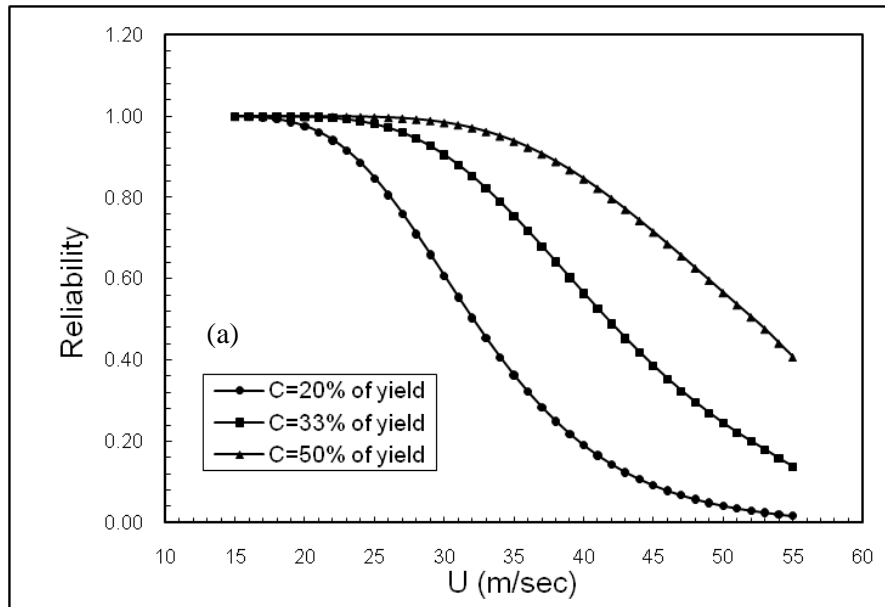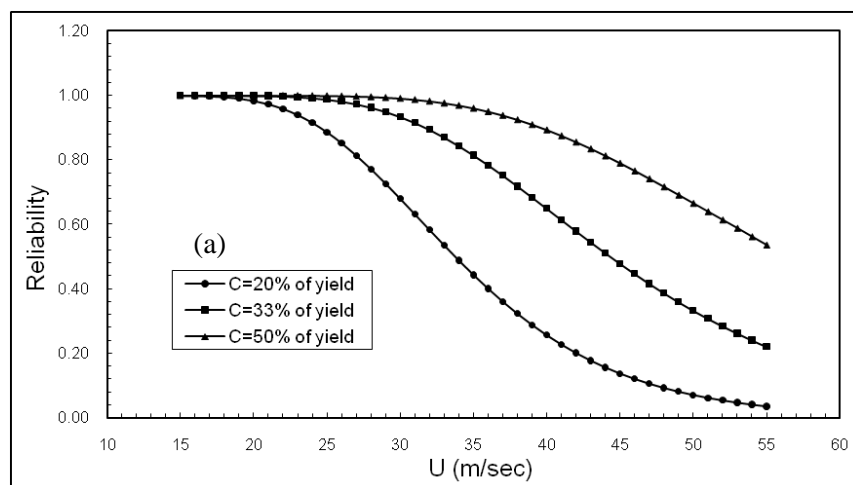
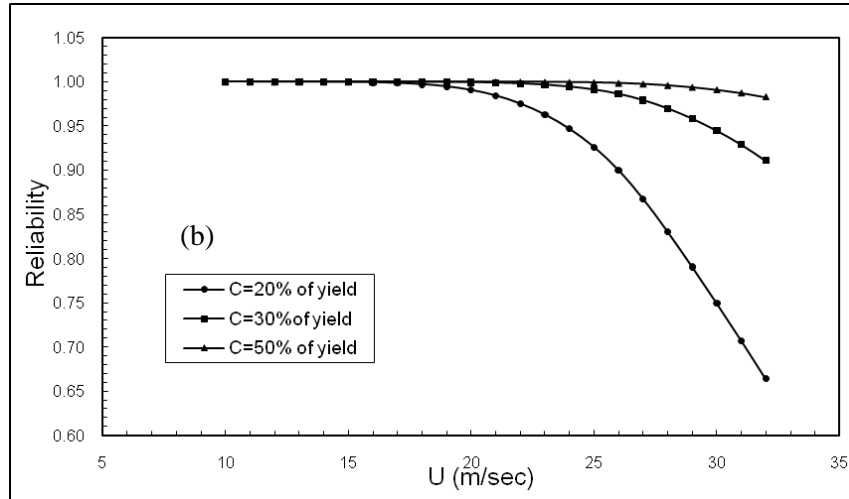*S. Pourzeynali, T.K. Datta / Comp. Meth. Civil Eng. 1 (2010) 15-35*

25

Figure 4. Effect of median value of capacity on reliability against buffeting failure, a) at node 5 for Thomas Bridge (μ=4; median F_8=1.25); b) at node 22 for Golden Gate Bridge (μ=4; median F_8=1.25).
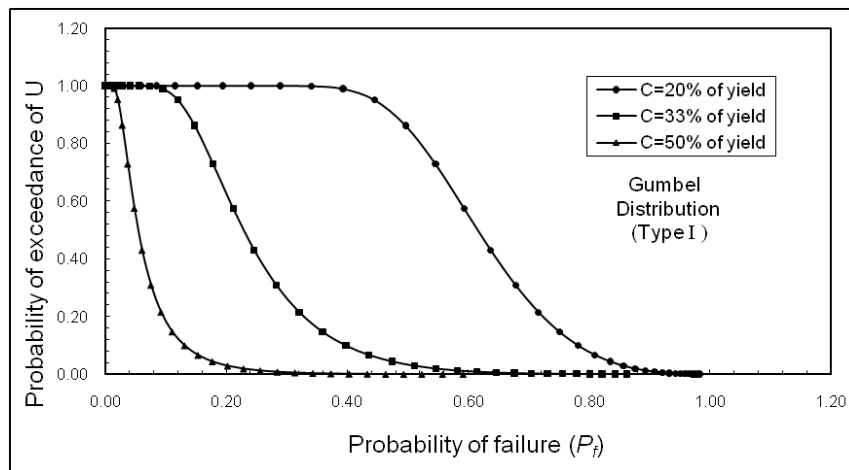
S. Pourzeynali, T.K. Datta / Comp. Meth. Civil Eng. 1 (2010) 15-35

26

Figure 5. Effect of median value of capacity on reliability against buffeting failure, a) at node 16 for Thomas Bridge (μ=4, median F_8=1.25); b) at node 5 Golden Gate Bridge (μ=4, median F_8=1.25).

Figure 6. Variation of P_f with exceedance probability of U (Thomas Bridge; μ=4, median F_8=1.25, U_{mean}=35, U_d=50m/sec).

6.1. Effect of the wind distribution on P_f

Since the buffeting response of the suspension bridges depends on the storm mean wind speed U at the bridge site, the probability of failure due to buffeting response, P_f, depends on the probability of U exceeding a certain value. This dependence is shown in Figures 6 to 11.

Figures 6 and 7 show the variation of $[1-F_u(U)]$ with P_f for the Thomas Suspension Bridge by assuming the Gumbel type I distribution and type II distribution [17] for the storm mean wind speed U, respectively. The figures are plotted for capacity C considered as 20%, 33% and 50% of yield stress σ_y. It is seen from the figures that P_f increases with the decrease in the value of the probability of exceedance. In addition, for a specified level of exceedance, the value of P_f, which is obtained from Gumbel type I distribution is more than that of the type II distribution. Further, P_f increases as capacity decreases.

Figures 8 and 9 show the same curves for Golden Gate Bridge. For this bridge, Gumbel type I distribution shows P_f to be less than that for the type II distribution. Further, P_f increases with the decrease in the value of probability of exceedance.

Figures 10 and 11 show the comparison between the results of P_f obtained by assuming Gumbel type I distribution and type II distribution for Thomas and Golden Gate Bridge, respectively. It can be seen from the figures that for Golden Gate Bridge type II distribution

S. Pourzeynali, T.K. Datta / Comp. Meth. Civil Eng. 1 (2010) 15-35

27

shows P_f more than the Gumbel distribution, whereas for Thomas Bridge, the Gumbel type I distribution shows P_f more than that of type II (when probability of exceedance is more than 20%).
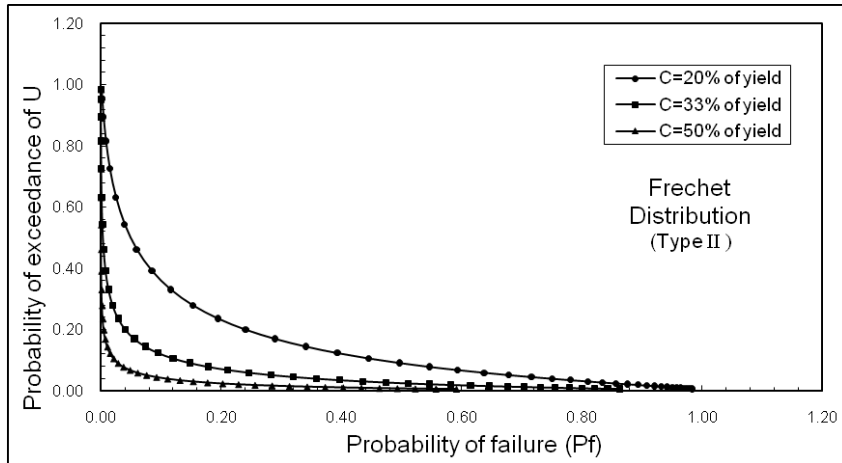

Figure 7. Variation of P_f with exceedance probability of U (Thomas Bridge; μ=4, median F_8=1.25, γ=5, β=20).
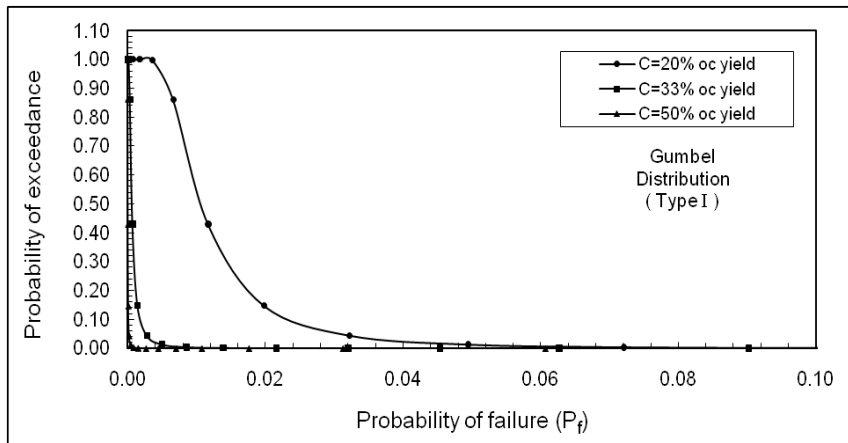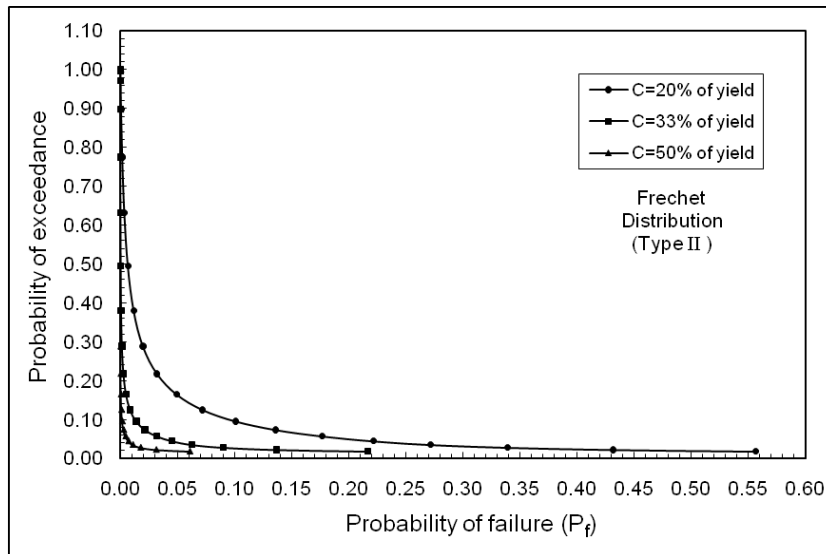

Figure 8. Variation of P_f with exceedance probability of U (Golden Gate Bridge; μ=4, median F_8=1.25; U_{mean}=20, U_d=30m/sec).

Figure 9. Variation of P_f with exceedance probability of U (Golden Gate Bridge; μ=4, median F_8=1.25; γ=7, β=18).

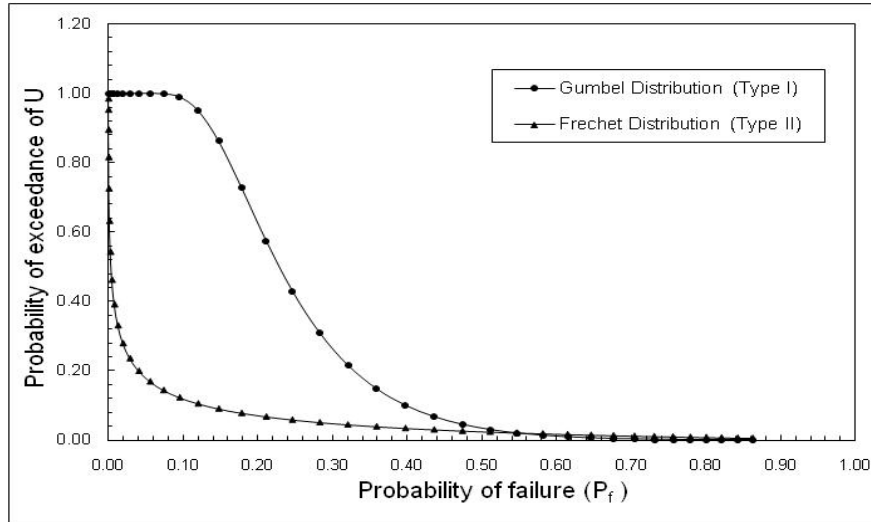*S. Pourzeynali, T.K. Datta / Comp. Meth. Civil Eng. 1 (2010) 15-35*

28

Figure 10. Comparison between P_f obtained by assuming wind distributions as Gumbel Type I and Type II (Thomas Bridge; C=33% of σ_y; γ=5, β=20; U_{mean}=35, U_d=50m/sec; μ=4; median F_8=1.25).
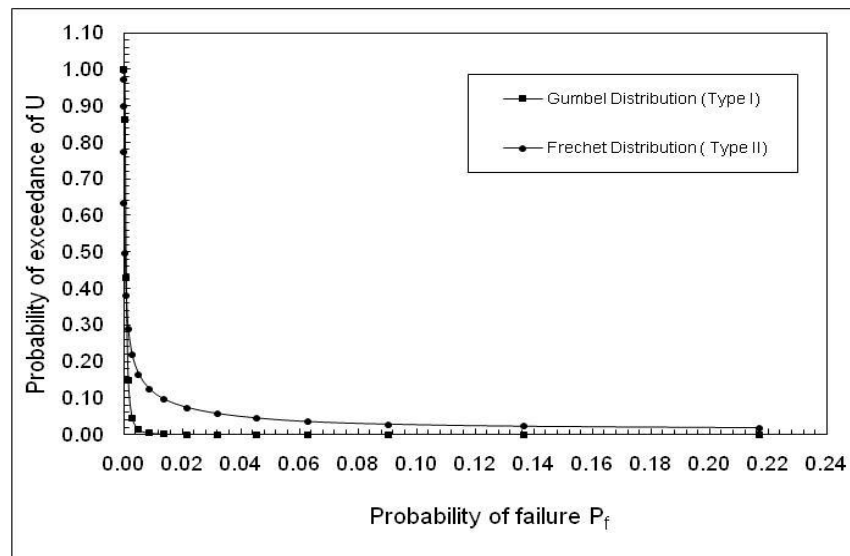

Figure 11. Comparison between P_f obtained by assuming wind distributions as Gumbel Type I and Type II (Golden Gate Bridge; C=33% of σ_y; γ=7, β=18; U_{mean}=20, U_d=30m/sec; μ=4; median F_8=1.25).

6.2. Effect of ductility factor on reliability against buffeting failure

Effect of ductility factor (μ) on reliability against buffeting failure is shown in Figures 12 and 13 for Thomas and Golden Gate Bridges, respectively. In the figures, reliability is plotted versus storm mean wind speed U. In order to evaluate reliability, capacity C is taken to be 50% of σ_y and median value of the factor F_8 is considered as 1.25. It can be seen from the figures, that μ has a significant effect on reliability. Reliability increases significantly with the increase in the value of ductility of the system. Further, it is seen from the figures that reliability rapidly decreases with the increase in the mean wind speed at the bridge site.
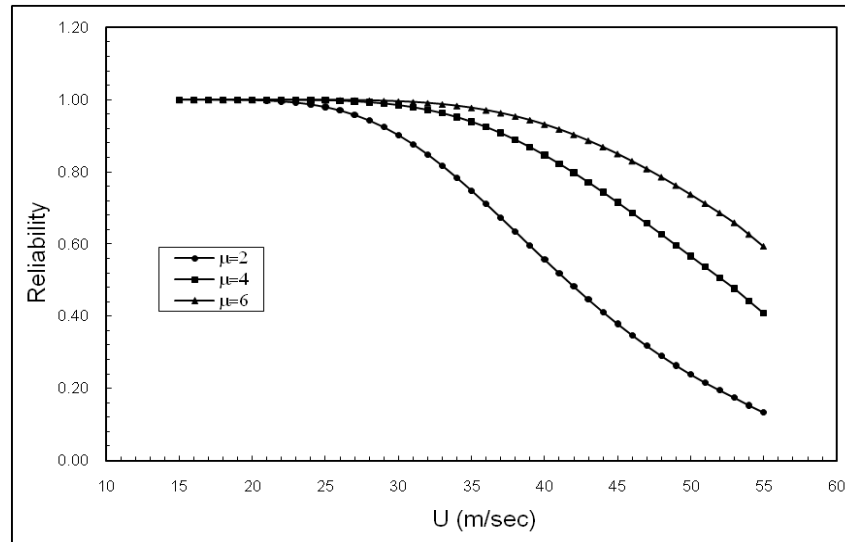
S. Pourzeynali, T.K. Datta / Comp. Meth. Civil Eng. 1 (2010) 15-35

29

Figure 12. Effect of ductility on reliability against buffeting failure (Thomas Bridge; C=50% of σ_y; median F_8=1.25).
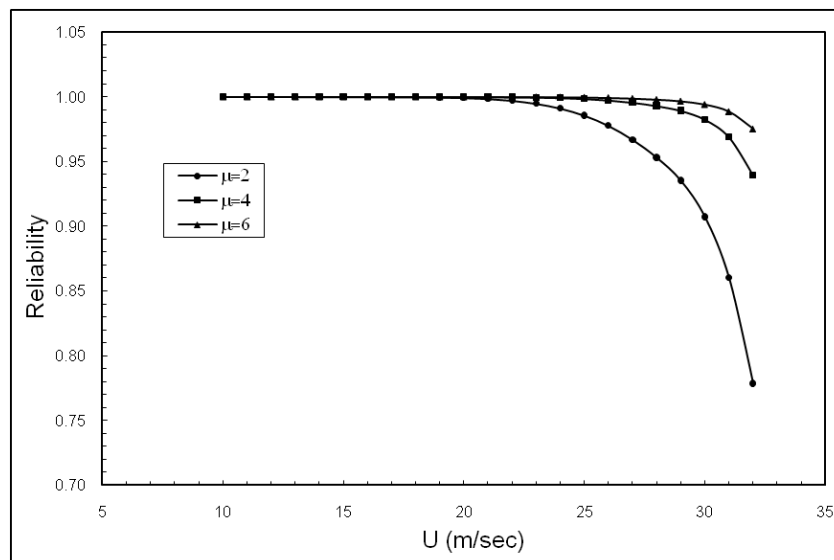

Figure 13. Effect of ductility on reliability against buffeting failure (Golden Gate Bridge; C=50% of σ_y; median F_8=1.25).

6.3. Effect of damage concentration factor on reliability against buffeting failure

Effect of the damage concentration factor on reliability of the Thomas and Golden Gate Bridge is shown in Figures 14 and 15, respectively. For evaluating the reliability, capacity of the system is taken about 50% of the yield stress σ_y and ductility of the system is considered as μ=4. Figures are plotted for three values of the median of the damage concentration factor F_8 about 0.75, 1.0 and 2.0. As it is seen from the figures, reliability significantly increases with the increase in the median value of F_8. When $\overline{F_8}$ increases from 0.75 to 2.0, for mean wind speed U=45 m/sec, reliability increases from 0.31224 to 0.93857 for Thomas Bridge.

30

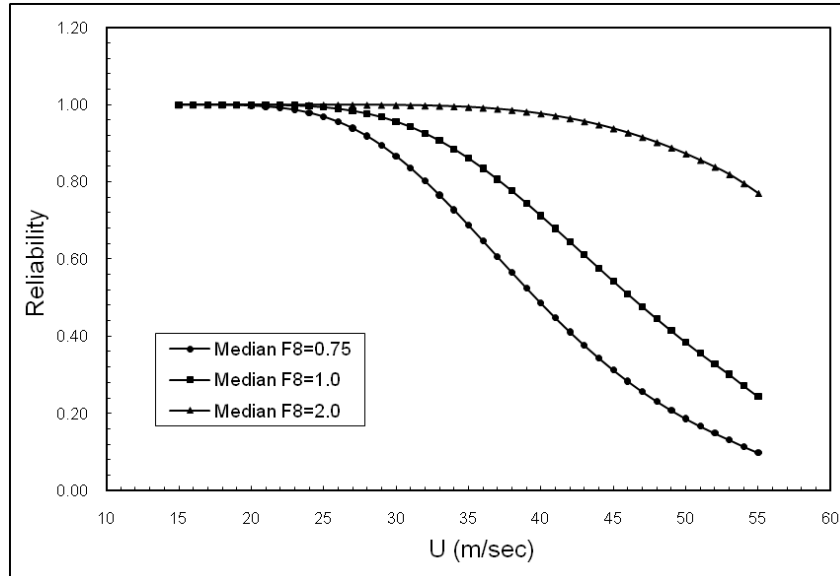*S. Pourzeynali, T.K. Datta / Comp. Meth. Civil Eng. 1 (2010) 15-35*

Figure 14. Effect of damage concentration factor on reliability against buffeting failure (Thomas Bridge; C=50% of σ_y, μ=4).
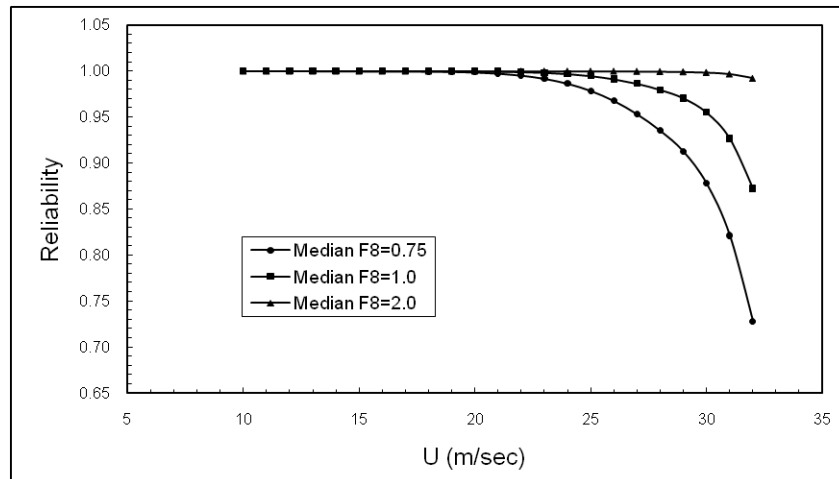

Figure 15. Effect of damage concentration factor on Reliability against buffeting failure (Golden Gate Bridge; C=50% of σ_y, μ=4).

6.4. Effect of damping ratio on reliability against buffeting failure

Figures 16 and 17 show the effect of structural modal damping ratio on reliability against buffeting failure for Thomas and Golden Gate Bridges, respectively. Figures are plotted for damping ratios of 1%, 3% and 5%. Further, capacity C is considered as 50% of σ_y, μ= 4 and $\widetilde{F}_8 = 1.25$. It can be seen from the figures that reliability against bending stress at the critical node of the bridge deck significantly increases with the increase in the value of damping ratio.
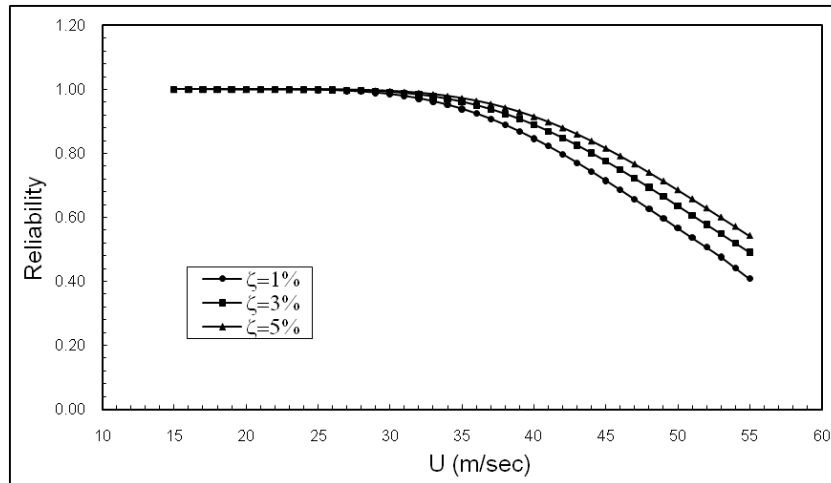
S. Pourzeynali, T.K. Datta / Comp. Meth. Civil Eng. 1 (2010) 15-35

31

Figure 16. mEffect of damping ratio on reliability against buffeting failure (Thomas Bridge; C=50% of σ_y, μ=4, median F_8=1.25).
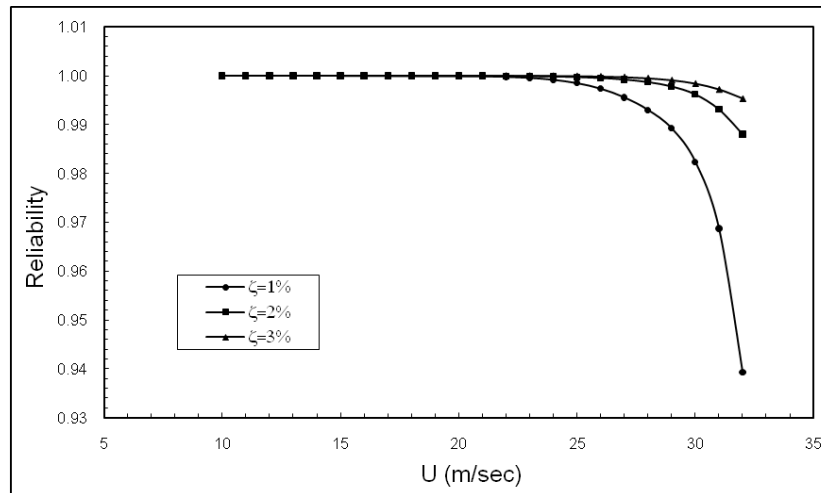

Figure 17. Effect of damping ratio on reliability against buffeting failure (Golden Gate Bridge; C=50% of σ_y, μ=4, median F_8=1.25).

6.5. Effect of number of storms on reliability against buffeting failure

In previous sections, reliability against buffeting failure due to bending stress is evaluated for a single storm having a certain mean wind speed U, and reliability is plotted versus U in the velocity range of interest for both bridges.

Since, number of storms ($\bar{n}$) in a year has a significant effect on P_f (equation (35)), the variation of reliability versus $\bar{n}$ is shown in Figures 18 and 19 for Thomas and Golden Gate Bridge, respectively. Reliability is evaluated at the critical nodes of the middle span and side span for both bridges. Figures show that for Thomas Bridge reliability changes nonlinearly with the number of storms ($\bar{n}$) in a year, whereas this variation almost remains linear for the Golden Gate Bridge.
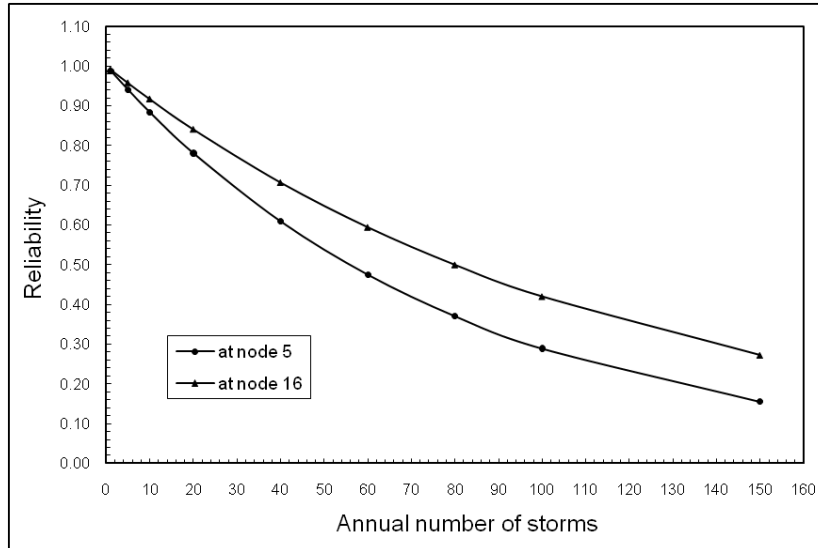
S. Pourzeynali, T.K. Datta / Comp. Meth. Civil Eng. 1 (2010) 15-35

32

Figure 18. Effect of annual number of storms on reliability against buffeting failure (Thomas Bridge; C=50% of σ_y, μ=4, median F_8=1.25).

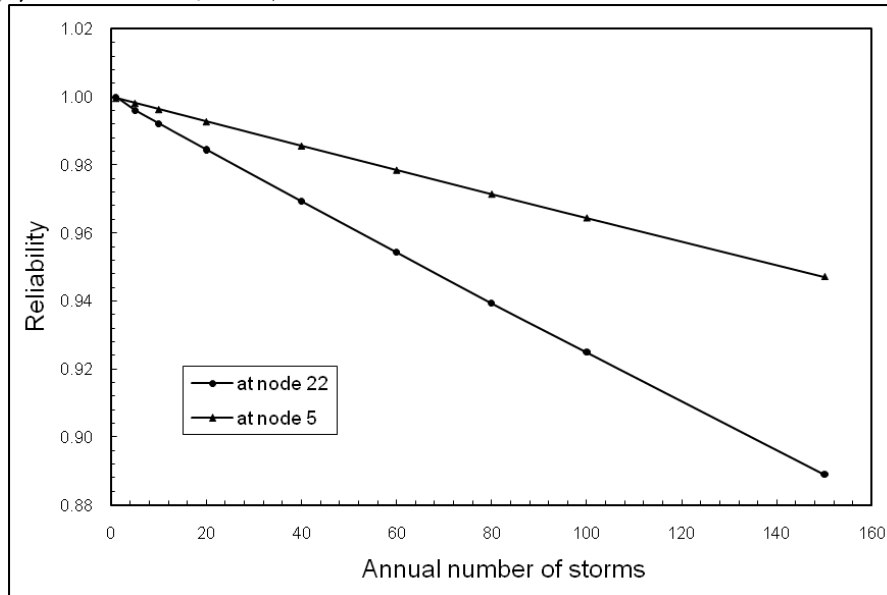Figure 19. Effect of annual number of storms on reliability against buffeting failure (Golden Gate Bridge; C=50% of σ_y, μ=4, median F_8=1.25).

7. Conclusions

The reliability of suspension bridges against buffeting failure is investigated. The reliability is estimated for uncertainties in stiffness and mass properties, modeling, damping and flutter derivatives of the deck cross section of the bridge. All uncertainty factors are assumed to be log-normally distributed random variables. The storm mean wind speed at the bridge site is assumed to follow Gumbel type I distribution or type II distribution given by Thom [17]. Using the concept of PRA procedure and the basic theory of reliability analysis, the results of the study on the Vincent-Thomas and Golden Gate Suspension Bridges show that:

    (i)   Probability of failure of the suspension bridges against bending stress significantly decreases with the increase in the value of the capacity of the system.

S. Pourzeynali, T.K. Datta / Comp. Meth. Civil Eng. 1 (2010) 15-35

33

(ii) Ductility and damage concentration factors for the bridges have significant effect on reliability against buffeting failure of the bridges.

(iii) Structural damping significantly influences the reliability against buffeting failure of the bridges.

(iv) Number of storms ($\bar{n}$) in a year significantly effects the reliability against buffeting failure of the bridges.

References

[1] Y.K. Lin, Motion of suspension bridge in turbulent winds, *Journal of the Engineering Mechanics Division*, American Society of Civil Engineers, ASCE, Vol. 105, 6 (1979) 921-932.

[2] R.H. Scanlan, H. Gade, Motion of suspension bridge spans under gusty wind, *Journal of the Structural Division*, American Society of Civil Engineers, ASCE, Vol.103, 9 (1977) 1867-1883.

[3] C.G. Bucher, Y.K. Lin, Stochastic stability of bridges considering coupled modes, *Journal of the Engineering Mechanics Division*, American Society of Civil Engineers, ASCE, Vol.114, 12 (1988) 2055-2071.

[4] R.H. Scanlan, N.P. Jones, Aeroelastic analysis of cable-stayed bridges, *Journal of Structural Engineering*, American Society of Civil Engineers, ASCE, Vol.116, 2 (1990) 279-297.

[5] Z.Q. Chen, The three dimensional analysis of behaviors investigation on the critical flutter state of bridges, *Proc. Symp. on Cable-Stayed Bridges*, Shanghai, China (1994) 10-13.

[6] N.P. Jones, R.H. Scanlan, Issues in the multimode aeroelastic analysis of cable-stayed bridges, Infrastructure '91, *Int. Workshop on Technology for Hong Kong's Infrastructure Devel.*, Commerical Press, Hong Kong (1991) 281-290.

[7] A. Namini, P. Albrecht, H. Bosch, Finite element-based flutter analysis of cable-suspended bridges, *Journal of Structural Engineering*, American Society of Civil Engineers, ASCE, Vol. 118, 6 (1992) 1509-1526.

[8] S. Pourzeynali, T.K. Datta, Buffeting Characteristics of Suspension Bridges, *Proc., International Conference on Advances in Wind and Structures, AWAS'02*, Pusan, Korea, (Aug. 21-23, 2002).

[9] S. Pourzeynali, T.K. Datta, Response of suspension bridges to aerodynamic excitation, *the 2nd International Conference on Structural Stability and Dynamics, ICSSD'02*, Singapore, (Dec. 16-18, 2002).

[10] S. Pourzeynali, T.K. Datta, Finite element based stability analysis of suspension bridges due to flutter, *Journal of Structural Engineering*, published by SERC Madras, India, Vol .30, No .2, (2003)101-110.

[11] A. Jain, N.P. Jones, R.H. Scanlan, Coupled flutter and buffeting analysis of long-span bridges, *Journal of Structural Engineering*, American Society of Civil Engineers, ASCE, Vol. 122, 7 (1996) 716-25.

[12] H. Katsuchi, N.P. Jones, R.H. Scanlan, Multimode coupled flutter and buffeting analysis of the akashi-kaikyo bridge, *Journal of Structural Engineering*, American Society of Civil Engineers, ASCE, Vol. 125, 1 (1999) 60-70.

[13] S. Mala, Safety and reliability of the cable system of a cable-stayed bridge under stochastic earthquake loading, *A thesis of Master of Engineering*, Asian Institute of Technology, AIT, Bankok, Thailand 1988.

[14] H.O. Madsen, P.O. Rosenthal, Wind criteria for long span bridges, *Proceedings of the International Symposium on aerodynamics of large bridges*, Copenhagen, Denmark, (Feb. 19-21, 1992).

S. Pourzeynali, T.K. Datta / Comp. Meth. Civil Eng. 1 (2010) 15-35

34

[15] D.E. Newland, An *Introduction to Random Vibrations, Spectral and Wavelet Analysis*, third edition, John Wiley & Sons, New York, 1993.

[16] S. Pourzeynali, T.K. Datta, Reliability analysis of suspension bridges against flutter failure, *International Journal of Sound and Vibration*, Vol. 254, No .1, (2002) 143-162.

[17] H.C.S. Thom, New distribution of extreme wind in the U. S., *Journal of the structural division*, ASCE, Vol. 94, 7 (1968) 1787-1801.

[18] S. Pourzeynali, Reliability analysis of suspension bridges for wind forces, *PhD. Thesis*, Indian Institute of Technology, Delhi, 2001.

[19] S. Pourzeynali, T.K. Datta, Reliability Analysis of suspension bridges against buffeting failure, *6th International Conference on Civil Engineering, ICCE2003*, Isfahan, Iran, (May 5-7, 2003).

[20] S. Pourzeynali, T.K. Datta, Conrol of flutter of suspension bridge deck using TMD, *International journal of Wind and Structure*, Vol .5, No .5, (2002) 407-422.

[21] A.M. Abdel-Ghaffar, Free torsional vibrations of suspension bridges, *Journal of the Structural Division*, American Society of Civil Engineers, ASCE, Vol. 105, 4 (1979) 767-789.

[22] A.M. Abdel-Ghaffar, Vertical vibration analysis of suspension bridges, *Journal of the Structural Division*, American Society of Civil Engineers, ASCE, Vol. 106,10 (1980) 2053-2074.

[23] Y.J. Ge, H.F. Xiang, H. Tanaka, Application of a reliability analysis model to bridge flutter under extreme wind, *Journal of Wind Engineering and Industrial Aerodynamics*, Vol. 86, 2-3 (2000) 155-167.

[24] E. Simiu, R.H. Scanlan, *Wind Effects on Structures,* second edition, John Wiley & Sons, Inc., New York, 1986.

[25] Committee on Fatigue and Fracture Reliability, Fatigue reliability: Variable amplitude loading, *Journal of the Structural Division*, American Society of Civil Engineers, ASCE, Vol. 108, 1 (1982) 47-69.

[26] A.G. Davenport, G.Larose, The structural damping of long span bridges: an interpretation of observation, *Presented at the Canada-Japan Workshop on bridge aerodynamics*, Ottawa, Canada, (Sept. 25- 27, 1989).

[27] R.H. Scanlan, J.J. Tomko, Airfoil and bridge deck flutter derivatives, *Journal of the Engineering Mechanics Division*, American Society of Civil Engineers, ASCE, Vol. 97, 6 (1971) 1717-1737.

[28] A. G. Davenport, Note on the distribution of the largest value of a random function with application to gust loading, *Journal Inst. Civil Engineering* 24 (1964) 187-196.

[29] M. Takeda, Y. Kai, M. Mizutani, A seismic PRA procedure in Japan and its application to a building performance safety estimation, Part 2: Fragility analysis, *proceeding of ICOSSAR '89, the 5th Int. Conference on Structural Safety and reliability*, San Francisco, (Aug. 7-11,1989).

S. Pourzeynali, T.K. Datta / Comp. Meth. Civil Eng. 1 (2010) 15-35

35

Appendix-I

The auto-power spectra of the wind velocity component *u* and *w*, which used in this study, are as follow [24]

$$S_{uu} = \frac{200\, z\, u_*^2}{U(1+50\, f)^{\frac{5}{3}}} \quad , \quad S_{ww} = \frac{3.36\, z\, u_*^2}{U\left(1+10\, f^{\frac{5}{3}}\right)} \quad , \quad f = \frac{n\, z}{U} \tag{I-1}$$

where *z* is the height of bridge deck above the ground; u_* is the friction velocity which is a function of surface roughness. In addition, the following empirical relationship is given for co-spectrum, C_{uw}, [11]

$$C_{uw} = -\frac{14\, z\, u_*^2}{U\left(1+9.6\, f\right)^{2.4}} \tag{I-2}$$

For quadrature spectrum, Q_{uw}, no relationship has yet been given [11], so it is assumed to be negligible.

The spanwise cross-spectral densities of the wind component can be written in conventional form as [24]

$$S\left(x_A,\, x_B\,, k\right) = S(k)\, e^{\frac{n\, c\, |x_A - x_B|}{U(z)}} \tag{I-3}$$

where $S(k)$ is ether $S_{uu}(k)$, $S_{ww}(k)$, or $S_{uw}(k)$; x_A and x_B are the *x* coordinates of the points along the bridge span at which the cross-spectrum is evaluated; *c* is the exponential decay coefficient for which the range is given by Jain et al. [11] as

$$8 \le c \le 16 \tag{I-4}$$

As well, the *uw*-wise spectrum of the wind velocity can be expressed as

$$S_{uw}(k) = C_{uw}(k) + i\, Q_{uw}(k) \tag{I-5}$$

in which co-spectrum and quadrature spectrum are given before.